

MODEL BASED BURNT GAS FRACTION CONTROLLER DESIGN OF DIESEL ENGINE WITH VGT/DUAL LOOP EGR SYSTEM

H. JUNG and S. CHOI*

School of Mechanical, Aerospace and System Engineering, KAIST, Daejeon 34141, Korea

(Received 21 August 2015; Revised 9 December 2015; Accepted 18 December 2015)

ABSTRACT—Recently, regulation of NOx and PM emission in diesel engines has become stricter and the EGR system has been expanded into a dual loop EGR system to increase EGR rate as well as to utilize exhaust gas strategically. In terms of engine combustion characteristics, burnt gas fraction is becoming an important factor of solving the NOx and PM emission reduction problem more efficiently but conventional controller focused only pressure and air flow rate targets. Unlike the previous studies, this paper describes a model based burnt gas fraction control structure for a diesel engine with a dual loop EGR and a turbocharger. Feedforward control inputs based on burnt gas fraction states aids in the precise control of diesel engines, especially in transient states by considering coupled behavior within the system. For the controller validation, a control oriented reduced order model of a diesel engine air management system is established to simplify the control input computation and its stability is proved by analysing the internal dynamics stability. Then, a sliding mode controller is designed and controller robustness at certain operating points is validated using an HiLS bench.

KEY WORDS : Nonlinear system, Reduced order model, Sliding mode control, Diesel engine air path system, Mean value model

NOMENCLATURE

EGR : exhaust gas recirculation
 VGT : variable geometry turbocharger
 m_1 : mass in the intake manifold (kg)
 m_2 : mass in the exhaust manifold (kg)
 m_3 : mass in the compressor upstream (kg)
 V_1 : volume of intake manifold (m^3)
 V_2 : volume of exhaust manifold (m^3)
 V_3 : volume of compressor upstream (m^3)
 V_d : engine displacement volume (m^3)
 F_1 : burnt gas fraction at intake manifold (-)
 F_2 : burnt gas fraction at exhaust manifold (-)
 F_3 : burnt gas fraction at compressor upstream (-)
 p_1 : pressure at intake manifold (kPa)
 p_2 : pressure at exhaust manifold (kPa)
 p_3 : pressure at compressor upstream (kPa)
 p_t : pressure at turbine downstream (kPa)
 p_a : ambient pressure (kPa)
 p_{lp} : pressure at upstream of low pressure egr valve (kPa)
 p_r : pressure ratio of valve downstream to valve upstream
 γ : specific heat ratio
 c_p : heat capacity at constant pressure
 R : ideal gas constant ($J\ kg^{-1}K^{-1}$)

P_t : turbine power (kW)
 P_c : compressor power (kW)
 J_{tc} : turbocharger inertia ($kg\cdot m^2$)
 N : turbocharger rotational speed (rad/s)
 N : engine RPM (rev/min)
 T_1 : temperature at intake manifold (K)
 T_2 : temperature at exhaust manifold (K)
 T_3 : temperature at compressor upstream (K)
 T_c : engine outlet temperature (K)
 T_{ic} : temperature after intercooler (K)
 T_{hpegr} : temperature after high pressure egr (K)
 T_{lpegr} : temperature after low pressure egr (K)
 T_a : ambient temperature (K)
 T_t : turbine outlet temperature (K)
 λ_s : stoichiometric ratio (-)
 \dot{m}_f : fuel mass flow rate (kg/s)
 \dot{W}_{ic} : mass flow rate which goes into cylinder (kg/s)
 \dot{W}_{ex} : mass flow rate which comes from cylinder (kg/s)
 \dot{W}_{hpegr} : high pressure egr mass flow rate (kg/s)
 \dot{W}_{lpegr} : low pressure egr mass flow rate (kg/s)
 \dot{W}_{air} : air mass flow rate (kg/s)
 \dot{W}_{vgt} : turbine mass flow rate (kg/s)
 \dot{W}_c : compressor mass flow rate (kg/s)
 C_d : discharge coefficient (-)
 η_t : turbine efficiency (-)
 η_c : compressor efficiency (-)
 η_m : turbocharger mechanical efficiency (-)
 η_{vol} : engine volumetric efficiency (-)

*Corresponding author. e-mail: sbchoi@kaist.ac.kr

1. INTRODUCTION

In accordance with strengthening emission gas regulations, an international effort is being undertaken to reduce hazardous contaminants such as Nitrogen Oxides (NO_x) and Particulate Matter (PM), which are the primary emissions of diesel engines (Upadhyay, 2001; Jung and Glover, 2003; Glenn, 2005; Wang, 2008; Lee, 2009). In terms of combustion, the Low Temperature Combustion (LTC) concept was adopted to solve the trade-off relationship problem of NO_x and PM emission, which depends on temperature. Additionally, after treatment systems such as Diesel Oxidation Catalyst (DOC) or Selective Catalytic Reduction (SCR) systems were developed to collect contaminants. And, the Exhaust Gas Recirculation (EGR) system was developed to help reduce contaminants by regulating the amount of air that goes into the cylinder. Among these systems, the EGR system is an effective one when considered in terms of its cost and its benefit.

There has been a steady stream of research into control of diesel engines using the VGT/EGR system. In the automotive industry, the map based control method is generally used; this method determines the feedforward term from a look-up table acquired by experimenting with the engine; then, remaining errors are eliminated using a feedback controller. However, this system requires consistent mapping work whenever the engine properties are changed.

Iwaware *et al.* (2009) suggested an intake pressure and compressor mass flow rate target based control scheme. This system, however, has a limitation in controlling NO_x and PM emissions because both targets control burnt gas fraction indirectly. Amstutz and Del Re (1995), Friedrich *et al.* (2009) suggested an EGR-rate model based control scheme. Although this model was meaningful because it used no additional sensors but its application was confined to only single loop EGR diesel engine.

Recent developments in the field of engine research have enhanced the analysis of engine behavior, enabling more accurate modeling of engines. Also, it has become possible to implement EGR-rate based control due to the introduction of the lambda sensor, which measures burnt gas fraction. Compared with original Mass Air Flow (MAF) and Manifold Air Pressure (MAP) sensor based controls, EGR rate based control helps to reduce undesirable transient responses such as overshoot and undershoot; it is known that NO_x and PM emissions are also reduced if undesirable peak response is eliminated in the transient range (Wang, 2008; Friedrich *et al.*, 2009; Castillo *et al.*, 2013).

Yan and Wang (2011) and Yan (2012) proposed a model based air path control scheme that worked by controlling burnt gas fraction, pressure, and temperature at the intake manifold. It showed quite good performance. However, the strategy of utilizing the Low Pressure EGR path is weak

because the three states are only related to intake manifold.

In this research, a model based burnt gas fraction control algorithm for a diesel engine with a VGT/Dual loop EGR system is developed. A diesel engine with a VGT/Dual loop EGR system is nonlinear. Also, VGT and EGR are physically coupled, that leads to a situation in which each system affects the other (Grondin, 2009). Compared with the conventional method of controlling the EGR rate indirectly using pressure and compressor mass flow rate as target states (Jung, 2003; Jin *et al.*, 2014; Kim, 2014), this research suggests a novel combination of target states including burnt gas fraction at the intake manifold, burnt gas fraction at the compressor upstream, and pressure at the exhaust manifold; this system can help control the EGR rate of the diesel engine air-path system directly. The model based controller can roughly track the desired value using feedforward control; feedback gains are set to eliminate remaining errors, with no attempt to deteriorate the transient response. With this model based approach, the accuracy of the feedforward term is critical.

The organization of this paper is as follows. The system description section describes the dynamics of the diesel engine air path system by applying the mean value model approximation. The model based controller design section deals with the mathematical analysis of the controller design. First, for computational simplicity, a reduced order model is obtained from the full model. Second, the control target strategy is introduced for precise burnt gas fraction control. After selecting the control targets, the stability of the system dynamics is proved. Then, the design method of the multi variable sliding mode controller is introduced. The simulation results section deals with HiLS (Hardware in the Loop Simulation) test results for dominant operating points of the diesel engine.

2. SYSTEM DESCRIPTION

2.1. Mean Value Modeling

The mean value modeling method is generally used in diesel engine air management systems to determine overall air flows using certain assumptions (Jung, 2003; Wahlström, 2006). State variables in each subsection are changeable within the combustion cycle, but control of the air flow needs to be dealt with in an overall view, which will allow the validity of mean value modeling. Assumptions for mean value modeling are as follows;

- Thermal loss by heat transfer is neglected (Adiabatic condition).
- Intake manifold volume, exhaust manifold volume, and compressor upstream volume are constant.
- Ideal gas constant and specific heat capacity ratio are constant.
- No pressure drop happens when gas passes cooler
- No residual mass exists in EGR path.

Figure 1 provides the schematic diagram of a turbo-charged diesel engine with a dual loop EGR system. Diesel

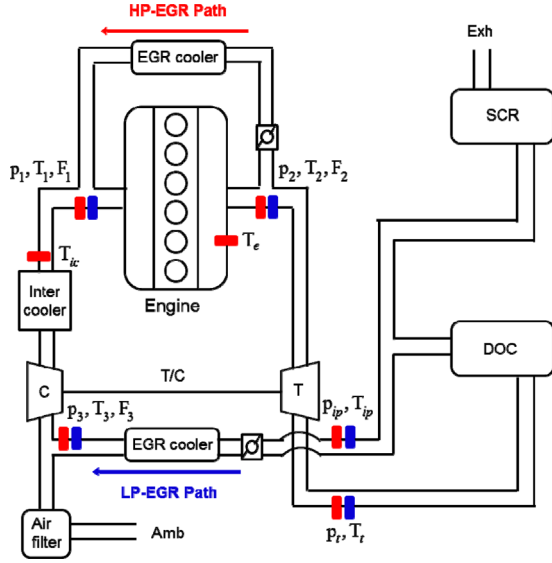


Figure 1. Diesel engine air management system structure.

engine air management system modeling for simulation was conducted based on a 6.0 L 6 cylinder heavy duty engine. For convenience, the intake manifold is denoted as subscript 1, the exhaust manifold as 2, and the compressor upstream as 3. The same subscripts that are used throughout this paper. For the model based controller design, it was assumed that pressure and temperature at some parts are measured, which is described in Figure 3.

2.2. Air Path Dynamics

In order to design a model based controller with high performance, accurate modeling of the system is required. However, high accuracy of the model leads inherently to increased computational quantity. The major contribution of this study is the introduction of the burnt gas fraction states and a simple burnt gas fraction dynamics model, especially for VGT/Dual loop EGR system, as target states of the controller model to reduce computation complexity as well as to regulate emission gas precisely.

The thermodynamic model for each section in Figure 1 can be obtained as follows;

From the mass conservation law, Equations (1) ~ (3) are obtained;

$$\dot{m}_1 = W_c + W_{\text{hpegr}} - W_{\text{ie}} \quad (1)$$

$$\dot{m}_2 = W_{\text{ex}} - W_{\text{hpegr}} - W_{\text{vgt}} \quad (2)$$

$$\dot{m}_3 = W_{\text{air}} + W_{\text{lpegr}} - W_c \quad (3)$$

where \dot{m}_1 , \dot{m}_2 and \dot{m}_3 are the change of mass in the intake manifold, exhaust manifold and compressor upstream each. W_c is the compressor mass flow rate. W_{hpegr} and W_{lpegr} are high pressure egr mass flow rate and low pressure egr mass flow rate each. W_{ie} is the mass flow rate which goes into cylinder and W_{ex} is the mass flow rate which comes

from cylinder. W_{vgt} is the turbine mass flow rate and W_{air} is the air mass flow rate.

From the energy conservation law and the ideal gas law, Equations (4) ~ (6) are obtained and temperature dynamics are obtained, as follows (Fengjun, 2012);

$$\dot{p}_1 = \frac{\gamma R}{V_1} (T_{\text{ic}} W_c + T_{\text{hpegr}} W_{\text{hpegr}} - T_1 W_{\text{ic}}) \quad (4)$$

$$\dot{p}_2 = \frac{\gamma R}{V_2} [T_e W_{\text{ex}} - T_2 (W_{\text{hpegr}} + W_{\text{vgt}})] \quad (5)$$

$$\dot{p}_3 = \frac{RT_3}{V_3} (W_{\text{lpegr}} + W_{\text{vgt}} + W_c) \quad (6)$$

$$\dot{T}_1 = \frac{RT_1}{p_1 V_1} [W_c (\gamma T_{\text{ic}} - T_1) + W_{\text{hpegr}} (\gamma T_{\text{hpegr}} - T_1)] \quad (7)$$

$$\dot{T}_2 = \frac{RT_2}{p_2 V_2} [W_{\text{ex}} (\gamma T_e - T_2) + W_{\text{vgt}} (T_2 - \gamma T_t) + \dots W_{\text{hpegr}} (T_2 - \gamma T_{\text{hpegr}})] \quad (8)$$

where p_1 , p_2 and p_3 are the pressure in the intake manifold, exhaust manifold and compressor upstream each. V_1 , V_2 and V_3 are the volume in the intake manifold, exhaust manifold and compressor upstream each. R is the ideal gas constant and γ is the specific heat ratio. T_{ic} is the temperature after intercooler. T_e is the engine outlet temperature. T_{hpegr} is the temperature after high pressure egr. T_t is the turbine outlet temperature. T_1 and T_2 are the temperature in the intake manifold and exhaust manifold each.

The burnt gas fraction indicates the concentration of burnt gas fraction of the control volume. Its dynamics is derived in the condition of mass conservation of each control volume (Jung *et al.*, 2014).

$$\dot{F}_1 = \frac{1}{m_1} (F_3 - F_1) W_c + \frac{1}{m_1} (F_2 - F_1) W_{\text{hpegr}} \quad (9)$$

$$\dot{F}_2 = \frac{W_{\text{ie}}}{m_2} F_1 - \frac{W_{\text{ie}} + \dot{m}_f}{m_2} F_2 + \frac{\dot{m}_f}{m_2} (1 + \lambda_s) \quad (10)$$

$$\dot{F}_3 = \frac{1}{m_3} [(F_2 - F_3) W_{\text{lpegr}} - F_3 W_{\text{air}}] \quad (11)$$

where F_1 , F_2 and F_3 are the burnt gas fraction in the intake manifold, exhaust manifold and compressor upstream each. λ_s is the stoichiometric ratio.

2.3. High Pressure/Low Pressure EGR Mass Flow Rate

The mass flow rate as gases pass through the EGR valves can be obtained using the orifice equation. The mass flow rate as gases pass from the valve upstream to the valve downstream can be written as follows;

$$W_{\text{egr}} = C_d A p_{\text{up}} \sqrt{\frac{2\gamma}{RT_{\text{up}}(\gamma-1)} \left[(p_r)^{\frac{2}{\gamma}} - (p_r)^{\frac{\gamma+1}{\gamma}} \right]} \quad (12)$$

where p_{up} and T_{up} are the pressure and the temperature at the upstream of the valve. $C_d A$ is usually expressed as the effective area. In modeling, experimental data for the effective area, depending on the EGR valve position, were used. The pressure ratio p_i is different whether the fluid is in sonic flow or not. p_i is determined as follows;

$$p_i = \max \left(\frac{p_{down}}{p_{up}}, \left(\frac{2}{\gamma + 1} \right)^{\frac{\gamma}{\gamma - 1}} \right) \quad (13)$$

where p_{down} is the pressure at the valve downstream.

2.4. Turbine and Compressor

The turbine and the compressor are interconnected through the turbine shaft. Therefore, relations between the turbine and the compressor are as follows;

$$\frac{d}{dt} \left(\frac{1}{2} J_{tc} n_{tc}^2 \right) = P_t - P_c \quad (14)$$

$$\dot{P}_c = \frac{1}{\tau_{tc}} (\eta_{tm} P_t - P_c) \quad (15)$$

where J_{tc} is the turbocharger inertia and n_{tc} is the turbine shaft angular velocity. P_t and P_c are turbine and compressor power each. τ_{tc} is the turbocharger time constant and η_{tm} is the turbocharger mechanical efficiency.

Turbine power is obtained as follows;

$$P_t = W_{vgt} c_p (T_2 - T_1) = W_{vgt} c_p \eta_t T_2 \left(1 - \left(\frac{p_t}{p_2} \right)^{\frac{\gamma - 1}{\gamma}} \right) \quad (16)$$

where c_p is the heat capacity at constant pressure. η_t is the turbine efficiency. p_t is the turbine outlet pressure.

Compressor power is obtained as follows;

$$P_c = W_c c_p (T_c - T_a) = W_c c_p \frac{1}{\eta_c} T_a \left(\left(\frac{p_c}{p_3} \right)^{\frac{\gamma - 1}{\gamma}} - 1 \right) \quad (17)$$

where T_a is the ambient temperature. η_c is the compressor efficiency. p_3 and p_c are pressure at compressor upstream and pressure at compressor downstream each.

Similar to the case of the EGR system, the turbine mass flow rate W_{vgt} is calculated based on the orifice equation. However, a modified orifice equation is usually applied for more accurate calculation, for which a look up table is included.

$$W_{vgt} = \frac{A p_2}{\sqrt{R T_2}} f_{\Pi_t}(\Pi_t) f_{vgt}(u_{vgt}) \quad (18)$$

$$f_{\Pi_t}(\Pi_t) = \sqrt{1 - \Pi_t^{K_t}} \quad (19)$$

where Π_t is the pressure ratio of the turbine upstream to downstream. Usually, K_t is set as a constant.

Equations (12), (13), (18) and (19) are important for composing an inverse orifice model, which will be dealt with later.

These modeling approaches are described in more detail in previous studies (Upadhyay, 2001; Jung, 2003; Wahlström, 2006; Jin *et al.*, 2014). In each paper, air path model is somewhat different depending on the hardware setup and the control volume location.

3. MODEL BASED CONTROLLER DESIGN

3.1. Controller Overview

An engine is a highly nonlinear and parameter varying system. In a nonlinear system, there are some approaches that have applied PID & optimal control schemes by locally linearizing the plant. In these cases, the controller should be designed by accomplishing loop shaping for all the engine characteristics (Wahlström, 2006). However, such a process is very complex and analysis would need to be done for various non-minimum phase behaviors of the engine. In addition, it is very difficult to analyze the system response in a MIMO system, which has various inputs. In this research, a controller was designed using the sliding mode control method. Not only does this approach consider the system nonlinearity, it is also robust against disturbances resulting from parametric uncertainty.

3.2. Control Oriented Reduced Order Model

By arranging the above equations, the full engine model can be obtained, as follows;

$$\begin{bmatrix} \dot{m}_1 \\ \dot{m}_2 \\ \dot{m}_3 \\ \dot{p}_1 \\ \dot{p}_2 \\ \dot{p}_3 \\ \dot{F}_1 \\ \dot{F}_2 \\ \dot{F}_3 \\ \dot{T}_1 \\ \dot{T}_2 \\ \dot{P}_c \end{bmatrix} = \begin{bmatrix} W_c + W_{hpegr} - W_{ie} \\ W_{ex} - W_{hpegr} - W_{vgt} \\ W_{air} + W_{lpegr} - W_c \\ \frac{\gamma R}{V_1} (T_{ic} W_c + T_{hpegr} W_{hpegr} - T_1 W_{ie}) \\ \frac{\gamma R}{V_2} [T_c W_{ex} - T_2 (W_{hpegr} + W_{vgt})] \\ \frac{R T_3}{V_3} (W_{lpegr} + W_{vgt} + W_c) \\ \frac{1}{m_1} (F_3 - F_1) W_c + \frac{1}{m_1} (F_2 - F_1) W_{lpegr} \\ \frac{W_e F_1 - W_e + \dot{m}_f}{m_2} F_2 + \frac{\dot{m}_f}{m_2} (1 + \lambda_s) \\ \frac{1}{m_3} [(F_2 - F_3) W_{lpegr} - F_3 W_{air}] \\ \frac{R T_1}{p_1 V_1} [W_c (\gamma T_{ic} - T_1) + W_{hpegr} (\gamma T_{hpegr} - T_1)] \\ \frac{R T_2}{p_2 V_2} [W_{ex} (\gamma T_c - T_2) + W_{vgt} (T_2 - \gamma T_1) + \dots \\ W_{hpegr} (T_2 - \gamma T_{hpegr})] \\ \frac{1}{\tau_{tc}} (\eta_{tm} P_t - P_c) \end{bmatrix} \quad (20)$$

Equation (20) is nonlinear and describes a high-order system of more than the 10th order, which makes system analysis difficult. In order to consider the simplicity of the controller computation, it is beneficial to construct a reduced order model of the dominant states. For this full model, mass flow dynamics can be included in the pressure dynamics. Although temperature is also important state for engine combustion, temperature state can be represented sufficiently with ideal gas law for steady state because its dynamic behavior is slow compared to that of other states and a slight error of the temperature states will not much affect the system response (Jung *et al.*, 2002). Thus, the control oriented reduced order model can be described as follows;

$$\begin{bmatrix} \dot{p}_1 \\ \dot{p}_2 \\ \dot{p}_3 \\ \dot{F}_1 \\ \dot{F}_2 \\ \dot{F}_3 \\ \dot{P}_c \end{bmatrix} = \begin{bmatrix} \frac{\gamma R}{V_1}(T_{ic}W_c + T_{hpegr}u_1 - T_1W_{ic}) \\ \frac{\gamma R}{V_2}[T_cW_{ex} - T_2(u_1 + u_2)] \\ \frac{RT_3}{V_3}(u_3 + W_{air} - W_c) \\ \frac{1}{m_1}(F_3 - F_1)W_c + \frac{1}{m_1}(F_2 - F_1)u_3 \\ \frac{W_{ic}}{m_2}F_1 - \frac{W_{ic} + \dot{m}_f}{m_2}F_2 + \frac{\dot{m}_f}{m_2}(1 + \lambda_s) \\ \frac{1}{m_3}[(F_2 - F_3)u_3 - F_3W_{air}] \\ \frac{1}{\tau_{ic}}(\eta_{tm}P_t - P_c) \end{bmatrix} \quad (21)$$

Here, the HP-EGR mass flow rate W_{hpegr} and the LP-EGR mass flow rate W_{pegr} , which are controlled by the EGR valves, were set to the control inputs u_1 and u_3 , respectively. Also, the turbine mass flow rate W_t , which is controlled by the turbine rack position, was set to the control input u_2 .

3.3. Control Target Selection Strategy

The proposed reduced order diesel engine air path system is still an under-actuated system, which means the number of control inputs is less than the system order. Thus, control targets should be strategically selected such that the controller can ensure the entire system stability by controlling some of the system states. Control targets were selected to design a model based burnt gas fraction controller, avoiding the use of turbine or compressor efficiency as a feed forward term. Having three actuator inputs, F_1 , F_3 , and p_2 were selected as control targets. F_1 is the principal factor in engine combustion characteristics because it determines the air to burnt gas ratio that flows through the cylinder. F_3 can be thought of as an assistant factor for precise burnt gas

fraction control because it determines the HP EGR to LP-EGR ratio. And, p_2 is a dominant factor from the aspect of both turbine mass flow rate and EGR mass flow rate.

3.4. Internal Dynamics Stability

The reduced order model is a 6th order system and there are three inputs. Thus, there exist internal dynamics in the model that are uncontrollable. Although there are uncontrollable states, they can naturally converge to an equilibrium point if the internal dynamics is stable.

Internal dynamics stability can be checked by using zero dynamics. First, we set \bar{y} for the target states;

$$\bar{y} = \begin{bmatrix} F_1 - F_{1d} \\ F_3 - F_{3d} \\ p_2 - p_{2d} \end{bmatrix} \quad (22)$$

If we apply steady state conditions,

$$\bar{y} = \dot{\bar{y}} = 0 \quad (23)$$

Then u_1 , u_2 , and u_3 are obtained as follows;

$$u_1 = \frac{F_3 - F_1}{F_2 - F_1}W_c \quad (24)$$

$$u_2 = \frac{T_cW_{ex}}{T_2} - \frac{F_3 - F_1}{F_2 - F_1}W_c \quad (25)$$

$$u_3 = \frac{F_3}{F_2 - F_3}W_{air} \quad (26)$$

By substituting the above inputs into the internal dynamics, stability can be verified.

3.4.1. Pressure at intake manifold

If we substitute Equation (24) into (4), it can be rearranged as follows;

$$\dot{p}_1 = \frac{\gamma R}{V_1} \left[\left(T_{ic} + T_{hpegr} \frac{F_3 - F_1}{F_2 - F_1} \right) W_c - \dots \right. \\ \left. \eta_{vol} \frac{NV_d}{120R} p_1 \right] \quad (27)$$

The coefficient of the term p_1 is negative, which implies that Equation (27) is stable.

3.4.2. Pressure at compressor upstream

If we substitute Equation (26) into (6), it can be rearranged as follows;

$$\dot{p}_3 = \frac{RT_3}{V_3} \left(W_{air} + \frac{F_3}{F_2 - F_3} W_{air} - W_c \right) \quad (28)$$

By applying the orifice equation, W_{air} can be expressed as a p_3 related term, followed by;

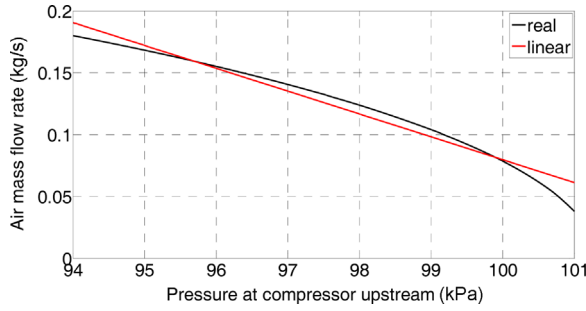


Figure 2. Linearization of air mass flow rate with pressure at compressor upstream.

$$W_{\text{air}} = C_d A p_a \sqrt{\frac{2\gamma}{RT_a(\gamma-1)} \left[\left(\frac{p_3}{p_a} \right)^{\frac{2}{\gamma}} - \left(\frac{p_3}{p_a} \right)^{\frac{\gamma+1}{\gamma}} \right]} \quad (29)$$

Then Equation (28) can be rearranged as follows;

$$\dot{p}_3 = \frac{RT_3}{V_3} \left[\left(1 + \frac{F_3}{F_2 - F_3} \right) C_d A p_a \times \sqrt{\frac{2\gamma}{RT_a(\gamma-1)} \left[\left(\frac{p_3}{p_a} \right)^{\frac{2}{\gamma}} - \left(\frac{p_3}{p_a} \right)^{\frac{\gamma+1}{\gamma}} \right]} - W_c \right] \quad (30)$$

where p_a is the ambient pressure and T_a the ambient temperature.

In Equation (30), it is not easy to check whether p_3 is stable or not because of its high nonlinearity. However, Equation (30) can be linearized because the range in which p_3 varies is not that large.

Figure 2 shows the air mass flow rate with pressure at the compressor upstream; it can be easily verified that Equation (30) is almost linear. By substituting all known values, Equation (30) can be linearized as follows;

$$W_{\text{air}} = -18.482 p_3 + 1927.9 \quad (31)$$

Then, Equation (28) can be simplified as follows;

$$\dot{p}_3 = \frac{RT_3}{V_3} \left[\left(1 + \frac{F_3}{F_2 - F_3} \right) \times (-18.482 p_3 + 1927.9) - W_c \right] \quad (32)$$

Thus, Equation (28) is stable.

3.4.3. Burnt gas fraction at exhaust manifold

There are no input terms in Equation (10). However, it is easily verified that Equation (10) is asymptotically stable because the coefficient of the F_2 term is negative.

3.4.4. Compressor power

If we substitute Equations (25) and (16) into (15), it can be

rearranged as follows;

$$\dot{P}_c = \frac{1}{\tau_{tc}} \left[W_{\text{ex}} c_p \eta_{\text{tm}} \eta_t T_e \left(1 - \left(\frac{P_t}{P_2} \right)^{\frac{\gamma-1}{\gamma}} \right) + \dots \right. \\ \left. \left(\frac{T_2 \eta_{\text{tm}} \eta_t \left(1 - \left(\frac{P_t}{P_2} \right)^{\frac{\gamma-1}{\gamma}} \right)}{T_a \left(\left(\frac{P_c}{P_3} \right)^{\frac{\gamma-1}{\gamma}} - 1 \right)} - 1 \right) P_c \right] \quad (33)$$

Usually F_1 is larger than F_3 since more burnt gas is added through the HP-EGR path. Also, $F_2 - F_1$ is larger than $F_3 - F_1$ and the efficiency terms η_{tm} , η_t are less than 1. Therefore, the part describe as (a) in Equation (33) is less than 1, and Equation (33) is stable.

3.5. Sliding Mode Control

It is not easy to apply a regular approach for the diesel engine air path model because the model not only contains time varying characteristics in state coefficients but also the system order is still high even though a reduced order model was designed. Thus, a multivariable sliding mode control scheme, which is quite easy to comprehend, was used to control the MIMO system.

First, sliding surfaces are defined as follows;

$$s_1 = F_1 - F_{1d} \quad (34)$$

$$s_2 = p_2 - p_{2d} \quad (35)$$

$$s_3 = F_3 - F_{3d} \quad (36)$$

A Lyapunov function is defined as follows;

$$V = \frac{1}{2} s_1^2 + \frac{1}{2} s_2^2 + \frac{1}{2} s_3^2 \quad (37)$$

The derivative of Equation (37) becomes negative definite if each derivative term is negative definite, i.e.

$$s_i \dot{s}_i < 0 \text{ for } i = 1 \sim 3 \quad (38)$$

Differentiating s_1 gives;

$$\dot{s}_1 = a W_{c,m} (F_3 - F_1) + a (F_2 - F_1) u_1 \dots - \dot{F}_{1d} + a \Delta W_c (F_3 - F_1) \quad (39)$$

where $a = \frac{1}{m_1}$ and subscript m denotes the modelled parameter value, which is distinguished from the real value.

Due to the limitation of sensor usage, the compressor mass flow rate W_c cannot be estimated accurately. Here, the unknown part is assumed to be upper bounded as follows;

$$|a\Delta W_c(F_3 - F_1)| \leq \delta_1 \quad (40)$$

Differentiating s_2 gives;

$$\dot{s}_2 = f[T_e W_{ex,m} + \Delta T_e W_{ex,m} + T_{e,m} \Delta W_{ex} \dots - T_2(u_1 + u_2)] - \dot{p}_{2d} \quad (41)$$

where $f = \frac{\gamma R}{V_2}$ and W_{ex} is determined from the following equation;

$$W_{ex} = \eta_{vol} \frac{m_1}{V_1} \frac{NV_d}{120} + \dot{m}_f \quad (42)$$

where $\eta_{vol}(p_1, N)$ is obtained from experimental data, which contains some uncertainty.

Here, the unknown part is assumed to be upper bounded as follows;

$$|\Delta T_e W_{ex,m} + T_{e,m} \Delta W_{ex}| \leq \delta_2 \quad (43)$$

Differentiating s_3 gives:

$$\dot{s}_3 = e_m[(F_2 + F_3)u_3 - F_3 W_{air}] + \dots \Delta e[(F_2 + F_3)u_3 - F_3 W_{air}] - \dot{F}_{3d} \quad (44)$$

where $e = \frac{1}{m_3}$.

Due to the lack of a temperature sensor at the compressor upstream, m_3 cannot be estimated accurately. Here, the unknown part is assumed to be upper bounded as follows;

$$|\Delta e[(F_2 + F_3)u_3 - F_3 W_{air}]| < \delta_3 \quad (45)$$

The control law u_1 , u_2 , and u_3 satisfying $s_1 \dot{s}_1 < 0$, $s_2 \dot{s}_2 < 0$ and $s_3 \dot{s}_3 < 0$ are suggested as follows;

$$u_1 = \frac{1}{a_m(F_2 - F_1)} [a_m W_{c,m}(F_1 - F_3) + \dot{F}_{1d} \dots - \lambda_1 \text{sgn}(s_1)] \quad (46)$$

$$u_2 = \left[\frac{1}{f_m} (\dot{p}_{2d} - \lambda_2 \text{sgn}(s_2) - T_e W_{ex,m}) \right] \left(-\frac{1}{T_2} \right) \dots - u_1 \quad (47)$$

$$u_3 = \frac{1}{e_m(F_{2m} - F_{3m})} [e_m F_{3m} W_{air} + \dots + \dot{F}_{3d} - \lambda_3 \text{sgn}(s_3)] \quad (48)$$

Here λ_1 , λ_2 , and λ_3 are chosen such that

$$\lambda_1 > \delta_1 \quad (49)$$

$$\lambda_2 > \delta_2 \quad (50)$$

$$\lambda_3 > \delta_3 \quad (51)$$

As for the controller design, a saturation function was used instead of a sign function, which is a common method to prevent chattering behavior of the sliding mode control. The saturation boundary was set at ± 0.02 for each burnt gas fraction value and at ± 5 (kPa) for the pressure value.

Figure 3 provides a diagram of the model based

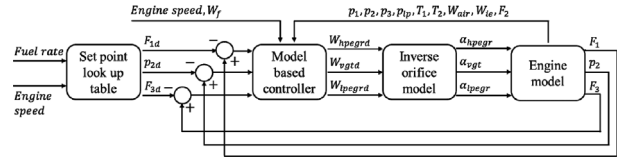


Figure 3. Diagram of model based controller of VGT/Dual loop EGR system.

controller. Actually, the number of sensors is limited for engine applications. Although the air mass flow rate can be measured using the MAF sensor, the compressor mass flow rate cannot be measured.

However, the compressor mass flow rate can be estimated indirectly if the LP-EGR mass flow rate can be estimated. To estimate the LP-EGR mass flow rate, pressure data is important at both the upstream and the downstream of the LP-EGR valve. For the controller application, it was assumed that the pressure at both of the upstream and downstream of the LP-EGR valve can be measured. And, the temperature at the downstream of the LP-EGR valve was held at a constant value.

The symbols W_{hpegrd} , W_{vgtd} and W_{lpegrd} in Figure 3 match with the control inputs u_1 , u_2 and u_3 each which are introduced in Equations (46) ~ (48). Actually, final control inputs should be EGR valve position and VGT rack position. Position value can be obtained from inverse orifice model which are designed using Equations (12) and (18). Given desired value of mass flow rate, effective area of pipe is obtained first. Then, EGR valve or VGT rack position are obtained from the map which transforms effective area to equivalent position.

4. SIMULATION RESULTS

4.1. Test Environments

The HiLS test is widely used in the industry for final simulation before experiments. HiLS results have high

Table 1. Engine specifications.

System specification	Unit	Value
Bore	mm	100
Stroke	mm	125
Number of cylinder	E.A.	6
Compression ratio	-	17.5
Firing order	-	1-5-3-6-2-4
Displacement volume	m ³	0.006
Intake manifold volume	m ³	0.001920
Exhaust manifold volume	m ³	0.0006352
Compressor upstream volume	m ³	0.0054
HP and LP EGR pipe diameter	mm	45

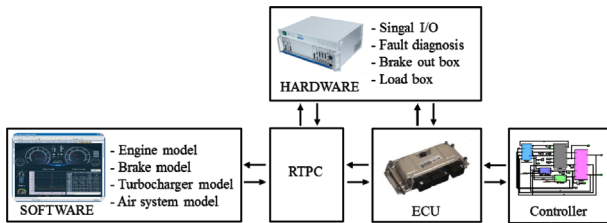


Figure 4. Organization of HiLS bench.

fidelity due to their reliably designed test bench. Figure 5 shows the layout of the HiLS bench with the product, which was developed and validated sufficiently for heavy duty diesel engine simulation (Jin *et al.*, 2014). Engine RPM, fuel injection timing, fuel injection rate, acceleration pedal torque, and brake torque are transferred to both of the hardware and software parts using INCAR software in an RTPC. The hardware part well depicts the engine operation, which means the engine can even halt given harsh operating conditions. From the engine sub-models, which are implemented in the software part, thermodynamic data like the pressure, temperature, and mass flow rate in each part are transferred to the controller through the ECU.

The controller calculates the desired actuator input and then transmits the feedback signal. For controller verification, AUTOBOX is connected to the HiLS bench via a CAN bus system. Figure 4 shows an organization of HiLS bench. The controller was validated with a sample time of 0.01 s. Also, the actuator bandwidth was set at 5 rad/s for the EGR valve and at 3.3 rad/s for the VGT actuator, to consider the actuator dynamics. Table 1 represents engine specifications of test bench.

4.2. Operating Points

Based on practical operating points of the heavy duty diesel engine, the five steady state engine RPM and fuel rate were set for the HiLS test. Beginning with an idle condition, the engine operates at either 1,400 RPM or 1,800 RPM while changing the fuel rate simultaneously. Figure 5 shows the operating points for the HiLS test. The trajectory was taken from the HiLS open loop test to get the reasonable transient rpm and fuel rate responses.

4.3. Desired Values of Target States

As for the desired values of the target states, experimental data for a heavy duty diesel engine were used. The exhaust manifold pressure and burnt gas fraction target look up tables were composed using open loop LTC experimental data of the pressure sensor, the temperature sensor in each part, and the MAF sensor while maintaining the engine operation in the steady state. Transient trajectory is obtained by interpolation.

4.4. HiLS Test Results and Discussion

Figures 6 and 7 show the controller verification results using the HiLS bench with different sliding mode gains.

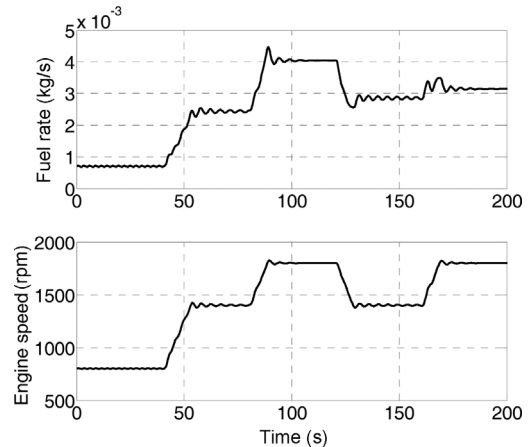


Figure 5. Operating points for VGT/Dual loop EGR HiLS test.

Table 2. Sliding mode controller gain.

Sliding mode gain	λ_1	λ_2	λ_3
Test 1	29.69	995	61
Test 2	32.96	995	71

Controller gains in each test are shown in Table 2.

The desired value of the burnt gas fraction values is almost held constant for the varying operating points, which is the characteristic of LTC. It is noteworthy that the sliding mode controller showed a quite smooth transient response since PM and NO_x are usually compounded during bad transient responses such as overshoot and undershoot of the burnt gas fraction states.

Although there exist parametric uncertainties such as in the volumetric efficiency, lack of pressure and temperature sensor data at certain parts, and ignored temperature dynamics in the reduced order model, the sliding mode controller showed a quite robust response for such model uncertainties. For test 1, the sliding controller showed a robust response for all operating points. The chattering of burnt gas fraction during the idle condition in Figure 6 (a) was due to the constant but excessive feedback gain which needs to be scheduled as a function of the operating conditions. Large chattering behavior during 120 ~ 130 seconds of the transient state in Figure 6 (a) was due to the coupling effect of the VGT/EGR system. For the above transient ranges, the exhaust pressure drops rapidly, which causes instant drop of the compressor power. At low compressor power, the LP-EGR rate is high because the enough air mass flow rate is not generated much on that condition. Thus, pressure drop causes instant increases of the burnt gas fraction of both the compressor upstream and the intake manifold. To improve the steady and transient responses, test 2 was conducted with larger gains. Then, the chattering behavior of the burnt gas fraction at the compressor upstream during 120 ~ 130 seconds was

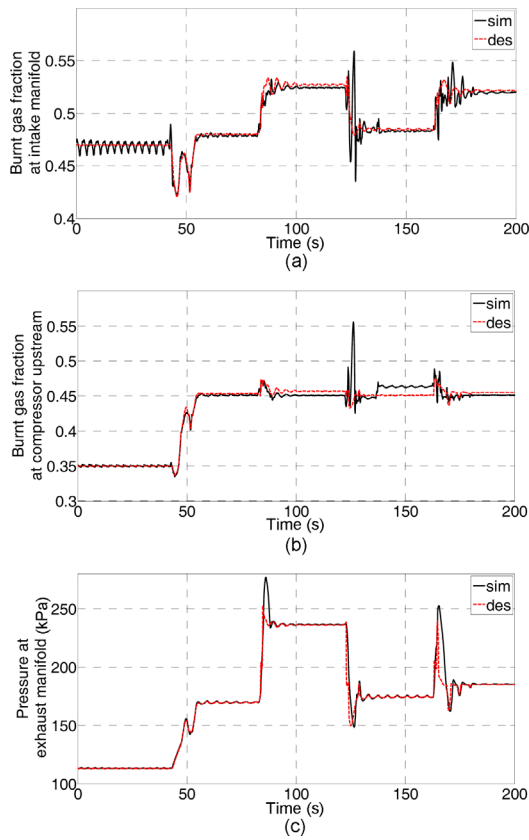


Figure 6. Test 1: Simulation results of model based feedback controller of VGT/Dual loop EGR HiLS bench: (a) Burnt gas fraction at intake manifold; (b) Burnt gas fraction at compressor upstream; (c) Pressure at exhaust manifold.

greatly reduced, which directly led to the reduction of the overshoot of the burnt gas fraction at the intake manifold. Also, for test 2, the steady state error of the burnt gas fraction at the compressor upstream was reduced, which can be verified in 80 ~ 160 seconds of Figure 7 (b). However, chattering behavior in the idle state got worse; also, there appeared small chattering behavior at the last operating point, with oscillatory motion of the EGR valve. Generally, sliding control with high enough feedback gains and appropriate saturation functions can narrow the boundary of steady state error but simply increased feedback gain can cause the chattering problem especially when it is combined with extra feedback delay. The chattering behavior during 0 ~ 40 seconds of Figures 7 (a) and (b) is due to the extra delay of the sensor signals which are inversely proportional to the engine operating speed. That kind of problems can be solved only by more accurate system modelling.

The RMS errors, excluding the idle conditions of both test 1 and 2, are listed in Table 3.

For the burnt gas fraction at the compressor upstream in test 1, the offset error at the steady state operating point is

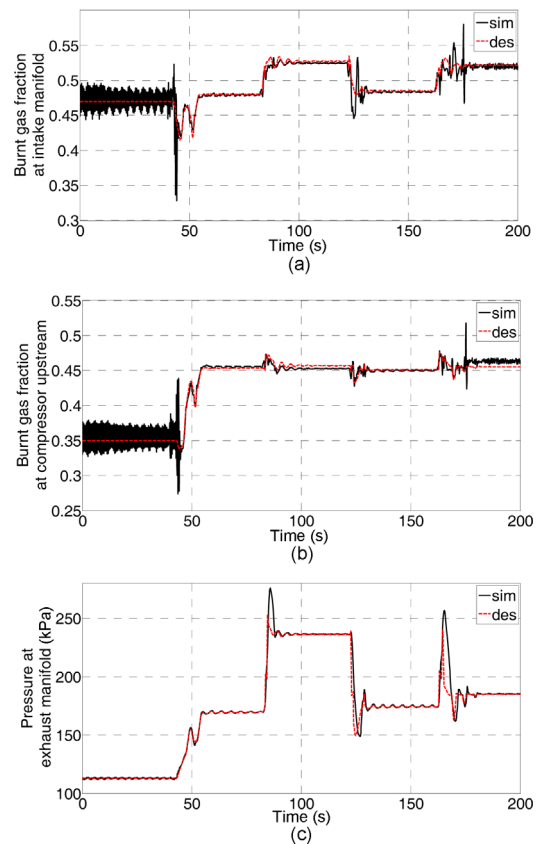


Figure 7. Test 2: Simulation results of model based feedback controller of VGT/Dual loop EGR HiLS bench: (a) Burnt gas fraction at intake manifold; (b) Burnt gas fraction at compressor upstream; (c) Pressure at exhaust manifold.

due to the uncertainty and the coupling effect of the air path system. Due to the lack of sensor usage, estimation of the LP-EGR mass flow rate cannot be accurate. Also, there is estimation error for the compressor mass flow rate, which may affect the feedforward control of the desired HP-EGR mass flow rate. Thus, the HP-EGR valve responded accordingly, which also affected VGT rack actuation due to the coupling effect.

Compared with the burnt gas fraction states, the pressure at the exhaust manifold showed consistent responses regardless of the variation of λ_1 and λ_3 values. By the nature of the air-path structure, HP-EGR and VGT are highly coupled. The main difference between test 1 and test 2 was the tracking performance of the burnt gas fraction at the compressor upstream. And, the consistent pressure response was due to the weak coupling effect between the LP-EGR path and the VGT system. The exhaust pressure tracking error was appeared during both tests when the desired trajectory of the exhaust manifold pressure dropped sharply during 80 ~ 90 and 160 ~ 170 seconds, which are shown by Figures 6 (b) and 7 (b). These lagging behaviors are due to turbocharger inertia and the limitation of rack

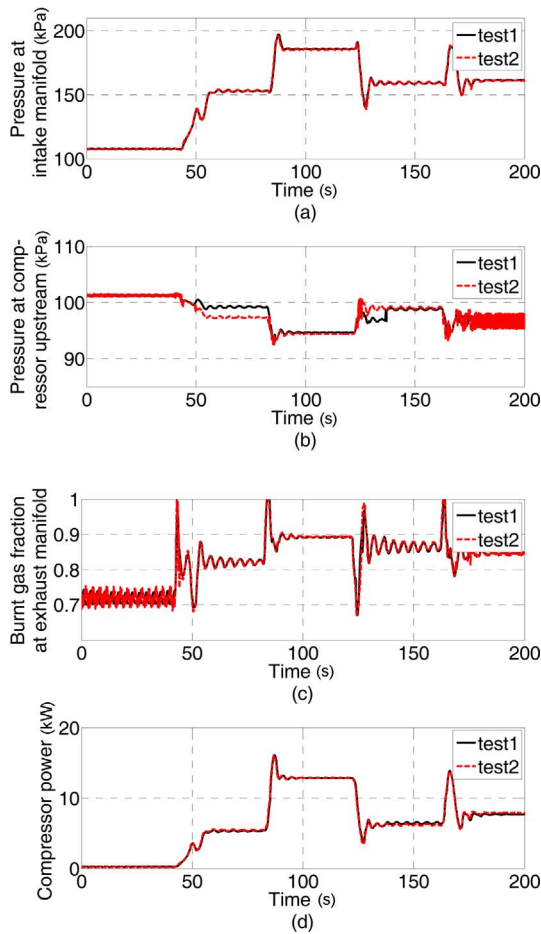


Figure 8. Simulation results of system internal dynamics in VGT/Dual loop EGR HiLS bench: (a) Pressure at intake manifold; (b) Pressure at compressor upstream; (c) Burnt gas fraction at exhaust manifold; (d) Compressor power.

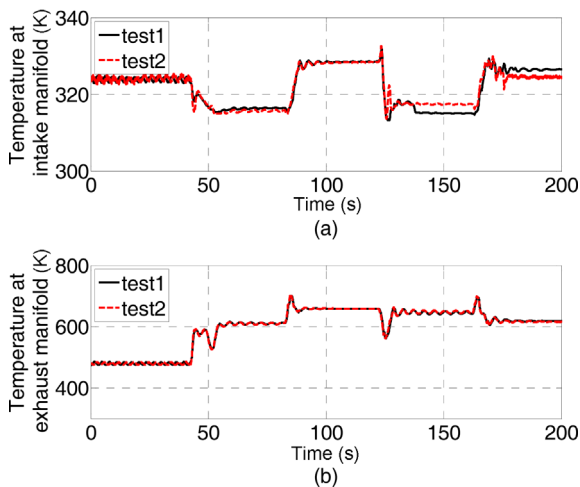


Figure 9. Simulation results of temperature in VGT/Dual loop EGR HiLS bench: (a) Intake manifold; (b) Exhaust manifold.

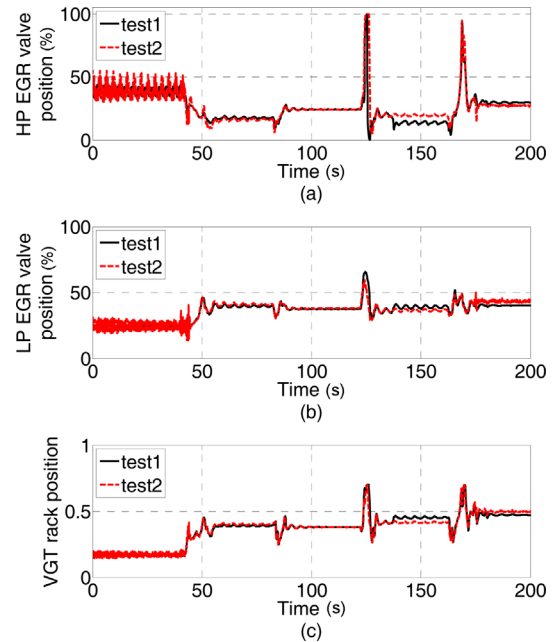


Figure 10. Simulation results of actuator response in VGT/Dual loop EGR HiLS bench: (a) HP EGR valve; (b) LP EGR valve; (c) VGT rack.

Table 3. RMS error of sliding mode controller.

RMS error	F_1	p_2	F_3
Test 1	1.66 %	3.83 %	2.26 %
Test 2	1.97 %	4.07 %	1.62 %

actuator bandwidth.

Figure 8 shows the behavior of the system internal states during the control; this figure confirms that all internal states show stable responses, as was proved in section 3.4. Although test 1 and 2 showed similar internal states responses, there were some discrepancies between test 1 and 2 at some operating points, which is due to steady-state error of target states. Differently from target states, internal states response is not of our interest as long as they are stable.

Figure 9 presents the temperature response at intake manifold and exhaust manifold respectively. They also showed similar results between test 1 and 2. Temperature values were also almost constant, which is a characteristic of LTC.

Figure 10 presents the EGR valve positions and VGT rack positions during the control. Except for the chattering behavior and some steady-state position difference which is due to the choice of feedback gain, both tests showed very similar responses.

5. CONCLUSION

A model based burnt gas fraction control scheme with a

certain combination of target states for heavy duty diesel engines was suggested in this research in order to reduce NO_x and PM emissions with a relatively simple computational logic compared with that of other state based controllers.

For robust controller design of the diesel engine air management system, the sliding mode control method was used. First, for controller simplicity, the control oriented reduced order model was organized from the engine model. The designed model based controller was validated with the HiLS bench. Through HiLS, implemental appropriacy in aspects of ECU implementation was also validated. Compared with conventional methods which take huge tuning efforts, the proposed controller took only constant gains through the operating points but, the designed controller showed quite robust performances and smooth transient responses except in certain severe transient conditions. The simple feed forward control terms were obtained from burnt gas fraction dynamics and gas pressure dynamics. However, due to the coupling effect of the air path system itself, feedforward term uncertainty at certain operating points cannot be removed perfectly.

Considering the results of tests 1 and 2, feedback gains should be designed just minimum enough to offset the disturbance of model uncertainties or sensor noise for the best performance of the sliding mode control. A relatively large feedback gain improved the transient response and reduced the offset error, but it caused excessive chattering behavior as expected. Although this research dealt with the sliding mode controller only, with simple constant feedback gains, the variable feedback control gain scheme which considers dynamic bandwidth of the system should be used to improve the transient response, among various operating points. Actually, there was a discrepancy between the full model and the reduced order model since the temperature dynamic model cannot be considered in the reduced order model. Considering these neglected dynamics and careful analysis and deep understanding of the air path system, a different control strategy that can compensate for the coupling effect effectively remains as a future work. Also, control target path generation strategy especially for transient trajectory should be carefully investigated to improve the transient responses.

ACKNOWLEDGEMENT—This research was supported by the MSIP (Ministry of Science, ICT and Future Planning), Korea, under the C-ITRC (Convergence Information Technology Research Center) (IITP-2015-H8601-15-1005) supervised by the IITP (Institute for Information & communications Technology Promotion). This work was supported by a National Research Foundation of Korea (NRF) grant funded by the Korean government (MSIP) (No. 2010-0028680).

REFERENCES

- Amstutz, A. and Del Re, L. R. (1995). EGO sensor based robust output control of EGR in diesel engines. *IEEE Trans. Control Systems Technology* **3**, 1, 39–48.
- Castillo, F., Witrant, E., Talon, V. and Dugard, L. (2013). Simultaneous air fraction and low-pressure EGR mass flow rate estimation for diesel engines. *5th IFAC Symp. System Structures and Control*.
- Friedrich, I., Liu, C. and Oehlerking, D. (2009). Coordinated EGR-rate model-based controls of turbocharged diesel engines via an intake throttle and an EGR valve. *IEEE Vehicle Power and Propulsion Conf.*, 340–347.
- Glenn, B. C. (2005). *Coordinated Control of the Turbo Electrically Assisted Variable Geometry Turbocharged Diesel Engine with Exhaust Gas Recirculation*. Ph. D. Dissertation. The Ohio State University, Ohio, USA.
- Grondin, O., Moulin, P. and Chauvin, J. (2009). Control of a turbocharged diesel engine fitted with high pressure and low pressure exhaust gas recirculation systems. *IEEE Conf. Decision and Control.*, 6582–6589.
- Iwadare, M., Veno, M. and Adachi, S. (2009). Multi-variable air-path management for a clean diesel engine using model predictive control. *SAE Paper No. 2009-01-0733*.
- Jin, H., Choi, S. and Kim, S. (2014). Design of a compressor-power-based exhaust manifold pressure estimator for diesel engine air management. *Int. J. Automotive Technology* **15**, 2, 191–201.
- Jung, H., Jin, H., Kim, S. and Choi, S. (2014). Simplified burnt gas fraction estimation for turbocharged diesel engine with dual loop EGR system. *Proc. IEEE Multi-Conf. Systems and Control*, 675–680.
- Jung, M. (2003). *Mean-value Modelling and Robust Control of the Airpath of a Turbocharged Diesel Engine*. Ph. D. Dissertation. University of Cambridge, Cambridge, UK.
- Jung, M. and Glover, K. (2003). Control-oriented linear parameter-varying modeling of a turbocharged diesel engine. *IEEE Conf. Control Applications*, 155–160.
- Jung, M., Ford, R. G., Glover, K., Collings, N., Christen, U. and Watts, M. J. (2002). Parameterization and transient validation of a variable geometry turbocharger for mean-value modeling at low and medium speed-load points. *SAE Paper No. 2002-01-2729*.
- Kim, S. (2014). *Model Based Coordinated Control of Dual-loop EGR and VGT in a Turbocharged Diesel Engine Air-path System*. M. S. Thesis. KAIST, Daejeon, Korea.
- Lee, B. (2009). *Dual-stage Boosting Systems: Modeling of Configurations, Matching and Boost Control Options*. Ph. D. Dissertation. The University of Michigan, Ann Arbor, USA.
- Upadhyay, D. (2001). *Modeling and Model based Control Design of the VGT-EGR System for Intake Flow Regulation in Diesel Engines*. Ph. D. Dissertation. The Ohio State University, Ohio, USA.
- Wahlström, J. (2006). *Control of EGR and VGT for Emission Control and Pumping Work Minimization in Diesel Engines*. M. S. Thesis. Linköpings Universitet, Linköping, Sweden.

- Wang, J. (2008). Air fraction estimation for multiple combustion mode diesel engines with dual-loop EGR systems. *Control Engineering Practice* **16**, **12**, 1479–1486.
- Wang, J. (2008). Hybrid robust air-path control for diesel engines operating conventional and low temperature combustion modes. *IEEE Trans. Control Systems Technology* **16**, **6**, 1138–1151.
- Yan, F. (2012). *Diesel Engine Advanced Multi-mode Combustion Control and Generalized Nonlinear Transient Trajectory Shaping Control Methods*. Ph. D. Dissertation. The Ohio State University. Ohio, USA.
- Yan, F. and Wang, J. (2011). Control of dual loop EGR air-path systems for advanced combustion diesel engines by a singular perturbation methodology. *American Control Conf.*, San Francisco, CA, USA, 1561–1566.